J Mol Model (2012) 18:4325–4332
DOI 10.1007/s00894-012-1445-9

ORIGINAL PAPER

Substitution, cooperative, and solvent effects on π pnicogen bonds in the FH_2P and FH_2As complexes

Xiu-Lin An · Ran Li · Qing-Zhong Li · Xiao-Feng Liu · Wen-Zuo Li · Jian-Bo Cheng

Received: 7 February 2012 / Accepted: 23 April 2012 / Published online: 9 May 2012

Abstract Ab initio calculations have been carried out to study the substitution effect on the π pnicogen bond in ZH_2P-C_2HM (Z=H, H_3C, NC, F; M=H, CH_3, Li) dimer, cooperative effect of the π pnicogen bond and hydrogen bond in XH-FH_2Y-C_2H_4 (X=HO, NC, F; Y=P and As) trimer, and solvent effect on the π pnicogen bond in FH_2P-C_2H_2, FH_2P-C_2H_4, FH_2As-C_2H_2, and FH_2As-C_2H_4 dimers. The interaction energy of π pnicogen bond increases in magnitude from -1.51 kcal mol^{-1} in H_3P-C_2H_2 dimer to -7.53 kcal mol^{-1} in FH_2P-C_2HLi dimer at the MP2/aug-cc-pVTZ level. The π pnicogen bond is enhanced by 12–30 % due to the presence of hydrogen bond in the trimer. The π pnicogen bond is also enhanced in solvents. The natural bond orbital analysis and symmetry adapted perturbation theory (SAPT) were used to unveil the source of substitution, cooperative, and solvent effects.

Keywords Cooperative effect · Enhancement · π pnicogen bond · Solvent effect · Substituents

Electronic supplementary material The online version of this article (doi:10.1007/s00894-012-1445-9) contains supplementary material, which is available to authorized users.

X.-L. An
The Laboratory of Theoretical and Computational Chemistry, College of Life Sciences, Yantai University, Yantai 264005, People's Republic of China

R. Li · Q.-Z. Li (✉) · X.-F. Liu · W.-Z. Li · J.-B. Cheng
The Laboratory of Theoretical and Computational Chemistry, School of Chemistry and Chemical Engineering, Yantai University, Yantai 264005, People's Republic of China
e-mail: liqingzhong1990@sina.com

Introduction

Intermolecular interaction plays a great role in molecular recognition, crystal engineering, and chemical reactions [1–3]. These roles are dependent to a great extent on its strength. The latter is related not only to the nature of atoms or groups participating directly in the intermolecular interactions but also with other factors such as substitution, cooperativity, and solvent effects. Due to the greater acidity, the proton of OH group in phenol forms a stronger hydrogen bond than that in water [4]. Because of the lower electronegativity of N, NH_3 is a stronger Lewis base than H_2O in hydrogen, lithium, and halogen bonds [5–7]. Ethylene is easier to provide electrons than acetylene [8] because the electrons in the sp^2 C atom are more far from the atomic nucleus and the constraint on them is smaller.

The substituted groups adjoined with the atoms or groups participating directly in the intermolecular interactions have a regulating effect on the strength of intermolecular interactions [9–11]. The electron-withdrawing groups in the Lewis acids play an enhancing role, while those in the Lewis bases have a weakening effect. The effect of electron-donating groups is reverse to that of electron-withdrawing ones. The methyl group is an interesting group and DNA methylation is an important phenomenon in biological systems [12]. Its roles in different types of intermolecular interactions have been studied systematically [13–15]. For example, in hydrogen-bonded complex of dimethylsulfoxide-methanol, the methyl group in dimethylsulfoxide is electron-donating and that in methanol is electron-withdrawing, both making a positive contribution to the formation of OH···O hydrogen bond [13].

The cooperativity is one of the most important properties of molecular interactions in biological systems [16] and molecular self-assembly [17]. Often binding of one molecule can enhance or reduce its affinity to bind subsequent

molecules. Such effects are in general referred to as "cooperativity". Because of its biological and chemical importance, cooperative effect has for a long time been attracting attention. A review for the cooperativity of intermolecular interactions has been presented by Alkorta et al. [18]. Many studies have been performed for cooperative effects in systems where two or more non-covalent interactions coexist [19–23]. The cooperativity in hydrogen bonding or σ-hole interactions is mainly induced by the polarization effect of the positive region by the negative site with which it is interacting [24, 25].

Solvent also has a prominent effect on the strength of intermolecular interactions. Its effect is different for different systems. The interactions in systems including ions and some stronger interactions may be weakened with the increase of solvent polarity [26–28]. An enhancing effect could occur for some weaker interactions [29]. The solvent effect can be studied by employing continuum models as well as molecular dynamics and Monte Carlo techniques.

It has been demonstrated that some group V molecules R_3X can interact with nucleophiles through the regions of positive electrostatic potentials found on their outer surfaces along the extensions of the R-X bonds [30]. Such interactions fall under the umbrella of σ-hole interactions, which are formed between the regions of positive electrostatic potentials found on covalently-bonded group IV-VII atoms and negative sites [31]. The tunability has been studied for σ-holes found on covalently-bonded group IV-VII atoms [32]. This is particularly notable for atoms which have more than one σ-hole [33]; how positive a σ-hole is can be altered by changing the substituent whose formation causes the σ-hole [34].

Recently, pnicogen bonding has been recognized as a new type of intermolecular interaction, which occurs between the pnicogen atom and the Lewis base site in another molecule. This interaction was proposed in a series of P···P complexes by Hey-Hawkins et al. [35]. They also studied a P···N interaction in an aminoalkyl- ferrocenyldichlorophosphane [36]. Other authors also focused their attention on this interaction [37–43]. This interaction has some similar properties with hydrogen and halogen bonds, but it shows some peculiar characteristics. Unlike halogen bonds, there is no requirement of a σ-hole of positive electrostatic potential on the P atom, nor is it necessary for the two interacting atoms to be of differing potential [38]. It should be noted that the electrostatic effects play an important role for the pnicogen bonding donor FH_2P studied in the present paper. In contrast to hydrogen bonds, the pertinent hydrogen is oriented away from, instead of toward, the N in H_3P-NH_3 dimer, and the N lone pair overlaps with the lobe of the P–H anti-bonding orbital [38]. In these studies of pnicogen bonds, the lone pair electrons in the Lewis bases bind with the pnicogen atoms. Given the ability of π electrons to form a hydrogen bond, they also form a π pnicogen bond with ethylene, acetylene, and benzene [41].

In this paper, we will study a series of π pnicogen bonded complexes involving ethylene and acetylene. FH_2P was selected as the pnicogen bonding donor because of its stronger binding with lone pair electrons [39]. For comparison with FH_2P, the FH_2As counterpart was also studied considering that FH_2As shows a positive region of electrostatic potential on the extension of the F-As bond [44]. Our aims are (1) to determine the structures, binding energies, and bonding characteristics of these complexes, (2) to examine the effect of substituents on the π pnicogen bonds, (3) to character the cooperative effect between the π pnicogen and hydrogen bonds, and (4) to study the solvent effect on π pnicogen bonds. We also performed an analysis for these complexes with natural bond orbital (NBO) and symmetry-adapted perturbation theory (SAPT) methods.

Theoretical methods

All complexes and the respective monomers have been optimized at the MP2/aug-cc-pVTZ level. Frequency calculations at the same level were carried out to confirm that the optimized structures are local minima on their potential surfaces. The frozen core (FC) approximation was applied in all calculations. All calculations were performed using Gaussian 09 program [45]. The interaction energy was calculated as a difference by subtracting the energy sum of the monomers from the total energy of the complex. The basis set superposition error (BSSE) was calculated with the counterpoise method of Boys and Bernardi [46] to correct the interaction energy. A single-point calculation was also performed at the CCSD(T)/aug-cc-pVTZ level on the MP2/aug-cc-pVTZ geometry.

The FH_2P-C_2H_2, FH_2As-C_2H_2, FH_2P-C_2H_4, and FH_2As-C_2H_4 complexes were optimized with a polarized continuum model (PCM) [47] at the MP2/aug-cc-pVTZ level. Natural bond orbital (NBO) analysis [48] was performed via the procedures within Gaussian 09. The interaction energy was decomposed with the symmetry adapted perturbation theory (SAPT) method using the SAPT2002 program [49]. The electrostatic potentials at the 0.001 electrons $Bohr^{-3}$ isodensity surfaces were calculated at the MP2/aug-cc-pVTZ level with WFA surface analysis suite [50].

Results and discussion

Substitution effect

It has been evidenced that the π systems of the various unsaturated hydrocarbon molecules (C_2H_2, C_2H_4, and C_6H_6) can serve as electron donors in π pnicogen bonds [41] and the strength of P···N pnicogen bond is affected greatly by substituents [39]. Thus we want to know if a

similar substitution effect is also present for π pnicogen bonds. Figure 1 shows the optimized structures of ZH_2P-C_2HM (Z=H, H_3C, NC, F; M=H, CH_3, Li) dimers. The structures are all rather similar, with the P-Z bond swung around away from the source of electrons. Their formation can be understood with electrostatic potentials of FH_2P and FH_2As shown in Fig. 2. It is found that the positive σ-holes on the extensions of the F-P and F-As bonds are more positive than those on the extensions of the H-P and H-As bonds. Some of the most important properties of these complexes are summarized in Table 1. The P atom is almost perpendicular to the C atom of the triple bonded HC≡CH in NCH_2P-C_2H_2 complex. It is turned to the C-H bond in H_3P-C_2H_2 and $(H_3C)H_2P$-C_2H_2 complexes and deflects to the C≡C bond in other complexes. The two free H atoms in ZH_2P are located at the same side with the triple bond. The P-Z covalent bond is in a line with the C atom in FH_2P-C_2HLi complex and is turned away from the P···C axis by 166.8–177.6 °.

The counterpoise-corrected interaction energies span the range of −1.51 kcal mol^{-1} for H_3P-C_2H_2 complex up to −7.53 kcal mol^{-1} for FH_2P-C_2HLi complex. They are arranged from up to down in order of increasingly negative in Table 1. It shows that the methyl group in the P subunit slightly strengthens the interaction with respect to an H atom, while the F substituent in the P subunit greatly enhances it. It is also expected that the enhancing effect of the nitro group is greater than that from the F atom in the π pnicogen bond like in the P···N pnicogen bonds [39]. The methyl group in the electron donor also strengthens the π pnicogen bond and its enhancing effect is better than that in the P subunit. The methyl effect here is similar to that in OH··· O hydrogen bond between dimethyl ether and methanol [51]. Surprisingly, the interaction energy amounts to −7.53 kcal mol^{-1} due to the Li substitution in the electron donor. It is about double as much as that in FH_2P-C_2H_2 complex. The prominent effect of alkali metal was also observed in halogen bonds [52]. The π pnicogen bond is stronger in the As complex than in the P analog due to the larger positive electrostatic potential on the As surface shown in Table 2. Ethylene forms a stronger π pnicogen bond than acetylene as expected.

Zero-point vibrational energies (ZPE) are added to the MP2/aug-cc-pVTZ values in the parentheses of Table 1. They result in a general reduction in the interaction energy by an amount of 0.91–1.92 kcal mol^{-1}. It is shown that ZPE has a prominent effect on the stability of the complexes. The H_3P-C_2H_2 complex has a positive energy. Even so, the stability of the complexes has an unchanged trend from one substituent to the next.

To ensure that the MP2 interaction energies are reliable, computations were also performed with the CCSD(T) method.

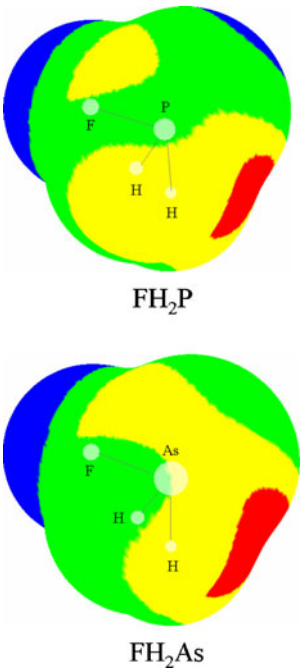

Fig. 2 Electrostatic potentials on the molecular surfaces of FH_2P and FH_2As molecules color ranges, in eV, are: red, greater than 004; yellow, between 004 and 002; green, between 002 and -001; blue, less than -001

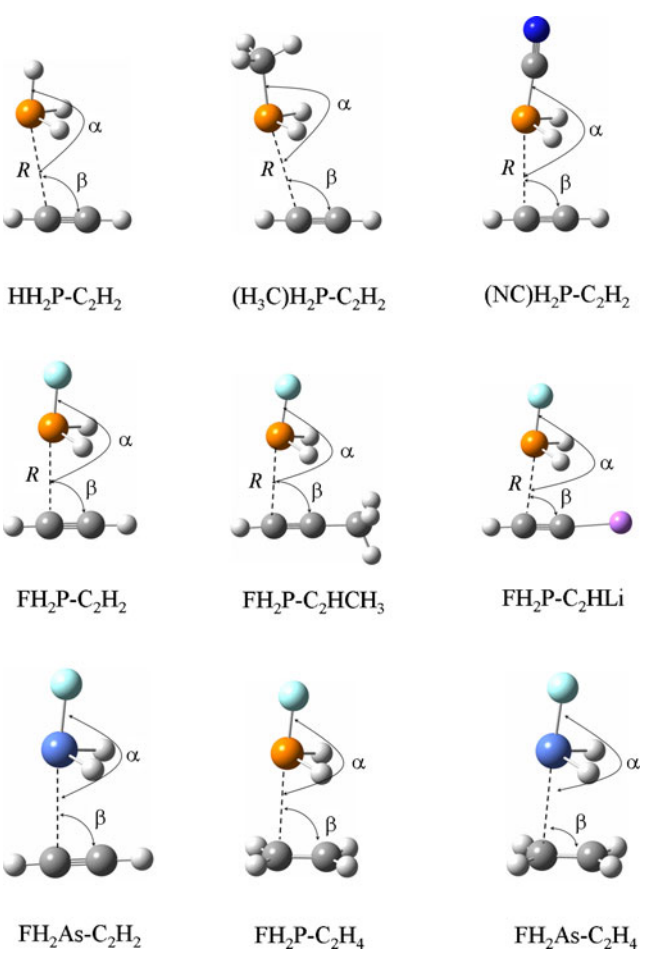

Fig. 1 The optimized structures of ZH_2P-C_2HM (Z=H, H_3C, NC, F; M=H, CH_3, Li), FH_2As-C_2H_2, FH_2P-C_2H_4, and FH_2As-C_2H_4 dimers

Table 1 Interaction energies (ΔE^{CP}, kcal mol^{-1}) corrected for BSSE, binding distance (R, Å), change of P-Z and As-F bond lengths (Δr, Å), bond angles (α and β, degree), and shift of P-Z and As-F stretch vibrations (Δv, cm^{-1}) in the ZH_2P-C_2HM (Z=H, H_3C, NC, F; M=H, CH_3, Li), FH_2As-C_2H_2, FH_2P-C_2H_4, and FH_2As-C_2H_4 dimers

	$\Delta E_{MP2}{}^{CP}$	$\Delta E_{CCSD(T)}{}^{CP}$	R	Δr	α	β	Δv
HH_2P-C_2H_2	−151(022)	−113	3424	0002	1668	989	−18
$(H_3C)H_2P$-C_2H_2	−157(−010)	−120	3394	−0000	1704	1049	2
$(NC)H_2P$-C_2H_2	−267(−105)	−209	3264	0005	1709	880	−9
FH_2P-C_2H_2	−362(−170)	−286	3017	0007	1776	859	−19
FH_2P-C_2HCH_3	−453(−362)	−359	2962	0010	1750	849	−30
FH_2P-C_2H_2Li	−753(−636)	−643	2835	0028	1798	831	−75
FH_2As-C_2H_2	−403(−213)	−313	3013	0011	1764	837	−22
FH_2P-C_2H_4	−407(−280)	−305	2915	0009	1793	856	−30
FH_2As-C_2H_4	−460(−341)	−337	2907	0015	1781	850	−31

Note: The interaction energies in parentheses are also corrected with zero-point vibrational energy (ZPE). The $\Delta E_{CCSD(T)}$ was obtained with a single-point calculation at the CCSD(T)/aug-cc-pVTZ level on the MP2/aug-cc-pVTZ geometry

The $\Delta E_{CCSD(T)}$ value was obtained with a single-point calculation at the CCSD(T)/aug-cc-pVTZ level on the MP2/aug-cc-pVTZ geometry. As expected, the MP2 method overestimates the interaction energy relative to the CCSD(T) one. The reduced percentage in the interaction energy is in a range of 15–25 % and becomes smaller for the stronger interaction.

The binding distance R in Table 1 is the distance between the P atom in ZH_2P and the C atom in C_2HM as shown in Fig. 1. It is decreased from 3.424 Å in H_3P-C_2H_2 complex to 2.835 Å in FH_2P-C_2HLi complex. This is consistent with the interaction energy. Upon complexation, the P-Z bond is elongated and the respective stretch exhibits a red shift in most complexes. NBO analysis shows that there is an orbital interaction between the C≡C bonding orbital and the anti-bonding P-Z orbital. The charge is transferred from the former to the latter. This accumulation of density in the antibonding orbital is responsible for the weakening of the P-Z bond.

As seen from Table 3, the NPA charge on Z is negative, while that on M is positive. The complexation leads to an increase for both the former and the latter. This means that Z is electron-withdrawing but M is electron-donating. The Δq_{CH3} in the pnicogen donor is larger in magnitude than the Δq_{CH3} in the pnicogen acceptor. This is not consistent with the size of their contribution in the formation of pnicogen bond.

For understanding the source of stability, we performed energy decomposition for these complexes. The SAPT components are presented in Table 4. The various terms follow the same trend as the total interaction energy except in $(H_3C)H_2P$-C_2H_2 complex. In this complex, the electrostatic contribution is a little smaller than the dispersion one, while in other complexes, the former is larger than the latter. The induction contribution is very small for Z=H, H_3C, and NC and becomes larger for Z=F. In all complexes, it is smaller than the electrostatic and dispersion terms. The methyl substituent in the electron donor leads to an increase in magnitude for all terms, while the reverse result is observed for the methyl substitution in the electron acceptor. The former brings out a more prominent effect on each term than the latter. The Li substituent in the electron donor causes a big increase for each term and its increased percentage climbs in magnitude from

Table 2 The most positive electrostatic potentials (V_{max}, kcal mol^{-1}) on the Y atom in FH_2Y (Y=P and As) monomer and its dimer XH-FH_2Y (X=HO, NC, and F) calculated at the MP2/aug-cc-pVTZ level

	$V_{s,max}$
FH_2P	4321
FH_2As	4987
FH-FH_2P	5370
FH-FH_2As	6093
HOH-FH_2P	4378
HOH-FH_2As	5157
NCH-FH_2P	5383
NCH-FH_2As	6011

Table 3 Stabilization energy (E^2, kcal mol^{-1}) due to the $\sigma_{(C\equiv C)} \rightarrow \sigma^*_{(Z\text{-}P(As))}$ orbital interaction and charge (q, e) on the Z and M in the ZH_2P-C_2HM (Z=H, H_3C, NC, F; M=H, CH_3, Li), FH_2As-C_2H_2, FH_2P-C_2H_4, and FH_2As-C_2H_4 dimers and its change (Δq, e) relative to the monomer

	E^2	q_Z	Δq_Z	q_M	Δq_M
HH_2P-C_2H_2	080	−0058	−0006	0226	0001
$(H_3C)H_2P$-C_2H_2	080	−0256	−0005	0225	0000
$(NC)H_2P$-C_2H_2	233	−0384	−0005	0231	0006
FH_2P-C_2H_2	426	−0635	−0013	0232	0007
FH_2P-C_2HCH_3	467	−0639	−0016	0041	0008
FH_2P-C_2H_2Li	1005	−0657	−0035	0921	0007
FH_2As-C_2H_2	662	−0681	−0020	0235	0010
FH_2P-C_2H_4	683	−0638	−0016	0177	0006
FH_2As-C_2H_4	1039	−0686	−0025	0180	0009

Table 4 Energy decomposition (in kcal mol^{-1}) in the ZH_2P-C_2HM (Z=H, H_3C, NC, F; M=H, CH_3, Li), FH_2As-C_2H_2, FH_2P-C_2H_4, and FH_2As-C_2H_4 dimers

	E_{elst}	E_{exch}	E_{ind}	E_{disp}	E_{int}^{SAPT2}
HH_2P-C_2H_2	−364	658	−023	−312	−041
$(H_3C)H_2P$-C_2H_2	−218	345	−019	−244	−136
$(NC)H_2P$-C_2H_2	−387	528	−059	−313	−231
FH_2P-C_2H_2	−682	985	−117	−454	−268
FH_2P-C_2HCH_3	−857	1264	−159	−592	−344
FH_2P-C_2H_2Li	−1803	2343	−431	−753	−644
FH_2As-C_2H_2	−849	1241	−191	−594	−393
FH_2P-C_2H_4	−972	1503	−189	−606	−265
FH_2As-C_2H_4	−1250	1954	−333	−683	−311

the dispersion term to the electrostatic term, and then to the induction term. A similar sequence is also found for the F substituent in the electron acceptor.

Cooperative effect

We also optimized the π pnicogen bond dimer of FH_2Y-C_2H_4 (Y=P and As) shown in Fig. 1 and then combined it with XH (X=HO, NC, F) through a H···F hydrogen bond. Figure 3 shows the optimized structure of XH-FH_2Y-C_2H_4 trimer. Its energetic parameters are collected in Table 5. The total interaction energy varies from −7.42 kcal mol^{-1} in HOH-FH_2P-C_2H_4 trimer to −11.51 kcal mol^{-1} in FH-FH_2As-C_2H_4 trimer. The FH_2As-C_2H_4 dimer is more stable than the FH_2P-C_2H_4 dimer. This is similar to that in H_3P-NH_3 and H_3As-NH_3 dimers [53]. The hydrogen bond is stronger in XH-FH_2As dimer than in XH-FH_2P one due to the smaller electronegativity of As element.

One sees from Table 5 that the addition of the H···F hydrogen bond to the FH_2Y-C_2H_4 dimer leads to a stronger π pnicogen bond. Similarly, the presence of the π pnicogen bond strengthens the H···F hydrogen bond inXH-FH_2Y dimer. The enhancement of the H···F hydrogen bond is larger than that of the π pnicogen bond. The stronger π pnicogen bond has a greater enhancing effect on itself and the H···F hydrogen bond, while the stronger H···F hydrogen bond also has a similar effect. This shows that the π pnicogen bond can interplay with the H···F hydrogen bond. The cooperative effect can be estimated with the cooperative energy. This term is calculated to be the difference between the total interaction energy in the trimer and the sum of the interaction energies for the π pnicogen bond and H···F hydrogen bond in the respective dimers. It is negative, indicating that both interactions have a positive cooperative effect. This value becomes larger for the stronger π pnicogen bond and H···F hydrogen bond. This effect is smaller than that between the halogen bond and hydrogen bond in H_3N-XY-

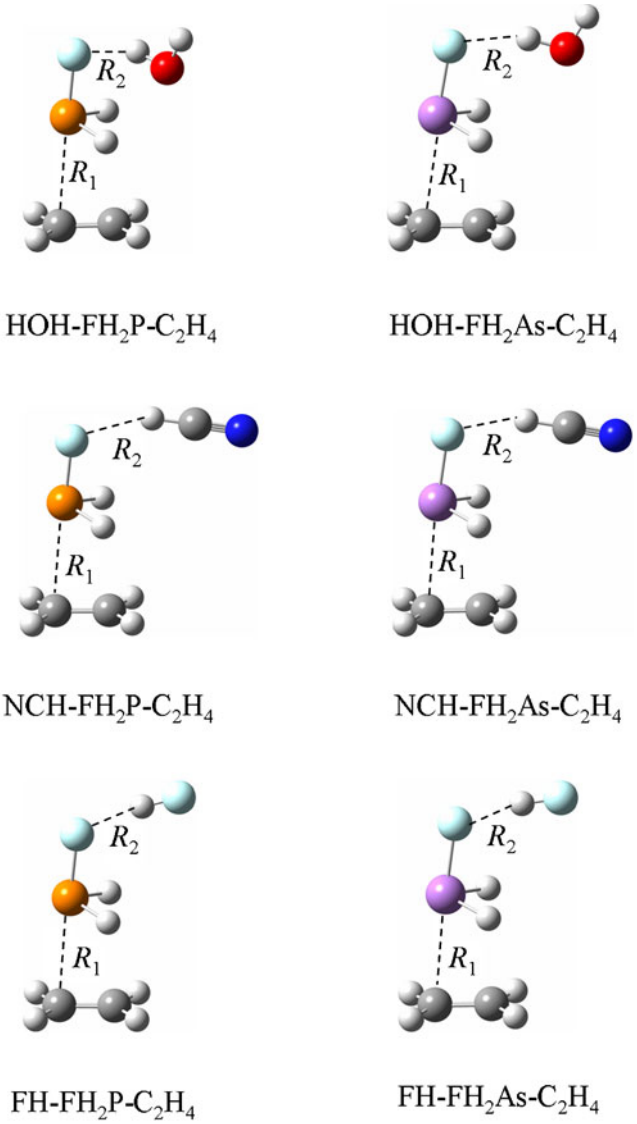

Fig. 3 The optimized structures of XH-FH_2Y-C_2H_4 (X=HO, NC, F; Y=P and As) trimers

HF (X, Y=F, Cl, Br) trimer [19]. A similar cooperative effect is also found in XH-FH_2Y-C_2H_2 (X=HO and F; Y=P and As) and NCH-FH_2As-C_2H_2 trimers shown in Table 5. However, the NCH-FH_2P-C_2H_2 trimer shows a cyclic structure (Fig. S1), which is different from the NCH-FH_2P-C_2H_4 trimer. In this complex, the interaction energies of pnicogen and hydrogen bonds are decreased and a positive cooperative energy is thus found.

The cooperativity between the π pnicogen bond and H···F hydrogen bond can also be reflected in the geometrical and spectroscopic changes. Table 6 presents the binding distances of the π pnicogen bond and H···F hydrogen bond in the complexes as well as their changes in the trimers relative to the dimers. Due to the stronger interaction, the binding distance of the π pnicogen bond is shorter in FH_2As-C_2H_4 dimer than in FH_2P-C_2H_4 dimer although the

Table 5 Total interaction energy (ΔE_{total}), interaction energies of pnicogen bond (ΔE_1) and hydrogen bond (ΔE_2), their increased percentage (%$\Delta\Delta E$), and cooperative energy (E_{syn}) in the XH-FH_2Y-C_2H_4 (X=HO, NC, F; Y=P and As) trimers All are in kcal mol^{-1}

	ΔE_{total}	ΔE_1	ΔE_2	%$\Delta\Delta E_1$	%$\Delta\Delta E_2$	E_{syn}
HOH-FH_2P-C_2H_4	−742	−455(−407)	−337(−290)	118	162	−045
HOH-FH_2As-C_2H_4	−889	−527(−460)	−442(−370)	146	195	−059
NCH-FH_2P-C_2H_4	−753	−496	−350(−265)	219	321	−081
NCH-FH_2As-C_2H_4	−920	−574	−476(−357)	248	333	−103
FH-FH_2P-C_2H_4	−923	−512	−522(−414)	258	262	−102
FH-FH_2As-C_2H_4	−1151	−598	−715(−560)	300	277	−132
HOH-FH_2P-C_2H_2	−696	−411(−362)	−336	135	159	−044
HOH-FH_2As-C_2H_2	−832	−470(−403)	−439	166	186	−059
NCH-FH_2P-C_2H_2	−741	−319	−177	−119	−332	089
NCH-FH_2As-C_2H_2	−859	−511	−468	268	310	−099
FH-FH_2P-C_2H_2	−863	−452	−505	249	220	−087
FH-FH_2As-C_2H_2	−1075	−521	−688	293	229	−112

Note: The data in the parentheses are from the respective dimer

As atom has a bigger atomic radius. The binding distance of the H···F hydrogen bond is also consistent with the interaction strength in the dimer. It can be seen that both types of the binding distances are shorter in the trimers, indicating that both interactions enhanced each other.

The change (Δr) of Y-F and X-H bond lengths are given in Table 7. The associated Y-F bond is lengthened in XH-FH_2Y dimer, while the free one is also elongated in FH_2Y-C_2H_4 dimer. The elongation of Y-F bond is larger in the former than in the latter. The $\Delta r_{Y\text{-}F}$ is 0.009 Å in FH_2P-C_2H_4 dimer and 0.015 Å in FH_2As-C_2H_4 dimer. One can see that the $\Delta r_{Y\text{-}F}$ in the trimer is larger than the sum of $\Delta r_{Y\text{-}F}$ in the respective dimers. For example, it is 0.028 Å in HOH-FH_2P-C_2H_4 trimer and the sum is 0.024 Å for HOH-FH_2P and FH_2P-C_2H_4 dimers. This is because the Y-F bond elongation is a combinative result of the π pnicogen bond and H···F hydrogen bond in the trimers. The X-H bond is also elongated in the trimer and dimer, and its elongation is also larger in the trimer. The red shift of the respective bond stretch frequency also shows a similar change.

The interaction energies of the π pnicogen bond and H···F hydrogen bond in the trimers were decomposed into four terms: electrostatic energy, exchanged energy, induction energy, and dispersion energy. It can be seen from Table 8 that all terms are increased in the trimers relative to the respective dimers. They have a larger increase in magnitude in the π pnicogen bond than in the H···F hydrogen bond. However, their increased percentage has some difference in different trimers. For the π pnicogen bond, it increases in order of dispersion energy<electrostatic energy<induction energy. A similar order is also found for the hydrogen bond in the H_2O trimer. For the hydrogen bond in other trimers, however, the electrostatic energy has the largest increased percentage, followed by the induction energy, and the dispersion energy shows the smallest increased percentage. The interaction of XH and F_2HY results in an increase of the most positive electrostatic potential on the Y atom surface given in Table 2, indicating that the electrostatic interaction is important in the enhancement of π pnicogen bond in the trimer.

Table 6 Binding distance of pnicogen bond (R_1) and hydrogen bond (R_2) as well as their change (ΔR) in the XH-FH_2Y-C_2H_4 (X=HO, NC, F; Y=P and As) trimers All are in Å

	R_1	R_2	ΔR_1	ΔR_2
HOH-FH_2P-C_2H_4	2869(2915)	2004(2061)	−0046	−0057
HOH-FH_2As-C_2H_4	2851(2097)	1904(1960)	−0056	−0056
NCH-FH_2P-C_2H_4	2853	2070(2090)	−0062	−0020
NCH-FH_2As-C_2H_4	2834	1974(2014)	−0073	−0040
FH-FH_2P-C_2H_4	2823	1746(1793)	−0092	−0047
FH-FH_2As-C_2H_4	2799	1665(1716)	−0108	−0051

Note: The data in the parentheses are from the respective dimer

Solvent effect

We selected FH_2P-C_2H_2, FH_2P-C_2H_4, FH_2As-C_2H_2, and FH_2As-C_2H_4 complexes as a model to study the solvent

Table 7 Change of Y-F and X-H bond lengths (Δr, Å) as well as shift of Y-F and X-H stretch vibrations (Δv, cm^{-1}) in the XH-FH_2Y-C_2H_4 (X=HO, NC, F; Y=P and As) trimers

	$\Delta r_{Y\text{-}F}$	$\Delta r_{X\text{-}H}$	$\Delta v_{Y\text{-}F}$	$\Delta v_{X\text{-}H}$
HOH-FH_2P-C_2H_4	0028(0015)	0003(0002)	−72(−29)	−29(−23)
HOH-FH_2As-C_2H_4	0039(0016)	0006(0004)	−72(−27)	−38(−32)
NCH-FH_2P-C_2H_4	0029(0013)	0002(0001)	−76(−26)	−39(−6)
NCH-FH_2As-C_2H_4	0039(0015)	0005(0003)	−72(−24)	−84(−52)
FH-FH_2P-C_2H_4	0040(0013)	0010(0007)	−97(−26)	−211(−158)
FH-FH_2As-C_2H_4	0052(0024)	0015(0011)	−94(−38)	−328(−241)

Note: The data in the parentheses are from the respective XH-FH_2Y dimer The $\Delta r_{Y\text{-}F}$ is 0009 Å in FH_2P-C_2H_4 dimer and 0015 Å in FH_2As-C_2H_4 dimer The $\Delta v_{Y\text{-}F}$ is -30 cm^{-1} in FH_2P-C_2H_4 dimer and -31 cm^{-1} in FH_2As-C_2H_4 dimer

Table 8 Energy decomposition (in kcal mol^{-1}) in the XH-FH_2Y-C_2H_4 (X=HO, NC, F; Y=P and As) trimer

	type	E_{elst}	E_{exch}	E_{ind}	E_{disp}	E_{int}^{SAPT2}
X=HO Y=P	P-bond	−1108(−136)	1701(198)	−238(−049)	−657(−051)	−304
	H-bond	−508(−075)	499(059)	−104(−020)	−202(−015)	−315
X=HO Y=As	P-bond	−1462(−212)	2281(327)	−444(−111)	−753(−070)	−378
	H-bond	−723(−120)	732(096)	−161(−034)	−254(−025)	−405
X=NC Y=P	P-bond	−1160(−269)	1757(393)	−268(−154)	−674(−085)	−345
	H-bond	−469(−138)	417(155)	−099(−027)	−204(−085)	−354
X=NC Y=As	P-bond	−1519(−188)	2347(254)	−487(−079)	−768(−068)	−427
	H-bond	−691(−174)	625(138)	−148(−036)	−261(−058)	−474
X=F Y=P	P-bond	−1246(−274)	1891(388)	−302(−113)	−693(−087)	−350
	H-bond	−829(−179)	799(138)	−273(−052)	−199(−024)	−502
X=F Y=As	P-bond	−1649(−399)	2564(610)	−559(−226)	−795(−112)	−439
	H-bond	−1183(−272)	1144(217)	−392(−084)	−254(−035)	−685

Note: The data in parentheses are the difference between in the trimer and in the dimer

effect on the π pnicogen bond. Calculations in solution were performed via the standard polarizable continuum model (PCM) [47] at the MP2/aug-cc-pVTZ level in two media with dielectric constants, 1.9 (heptane) and 4.9 (chloroform). The energetic, geometrical, and spectroscopic data are collected in Table 9. With the increase of dielectric constants, the binding distance is shorter, the elongation of F-P and F-As bonds is larger, and the red shift of F-P and F-As stretch vibrations is increased. These results show that the π pnicogen bond becomes stronger in solvent. However, the interaction energy in solution calculated with a similar method like in gas phase is decreased with the increase of dielectric constants. This is not consistent with the geometrical and spectroscopic data in solution. Such inconsistency in solution has been reported before [54]. Thus we calculated the interaction energy in solution by subtracting the energy sum of the monomers from the energy of dimer with all of them frozen in the geometry in solution. One sees from Table 9 that it becomes more negative in solution although the change is small, supporting the stronger π pnicogen bond in solvents. Additionally, this can also be evidenced by the strength of the π pnicogen bond in the HOH-FH_2P-C_2H_4 and HOH-FH_2As-C_2H_4 trimers.

Table 9 The interaction energy (ΔE^{CP}, kcal mol^{-1}) corrected for BSSE, binding distance (R, Å), change of P-F and As-F bond lengths (Δr, Å), and frequency shift of P-F and As-F stretch vibrations (Δv, cm^{-1}) for FH_2P-C_2H_2, FH_2P-C_2H_4, FH_2As-C_2H_2, and FH_2As-C_2H_4 dimers in different media

		Gas	Heptane	Chloroform
FH_2P-C_2H_2	ΔE^{CP}	−362	−368	−370
FH_2P-C_2H_4	ΔE^{CP}	−407	−417	−418
FH_2As-C_2H_2	ΔE^{CP}	−403	−413	−414
FH_2As-C_2H_4	ΔE^{CP}	−460	−474	−476
FH_2P-C_2H_2	R	3017	3012	3011
FH_2P-C_2H_4	R	2915	2093	2890
FH_2As-C_2H_2	R	3013	2992	2972
FH_2As-C_2H_4	R	2907	2873	2841
FH_2P-C_2H_2	Δr	0007	0007	0008
FH_2P-C_2H_4	Δr	0009	0011	0012
FH_2As-C_2H_2	Δr	0011	0013	0015
FH_2As-C_2H_4	Δr	0015	0019	0024
FH_2P-C_2H_2	Δv	−19	−21	−28
FH_2P-C_2H_4	Δv	−30	−38	−40
FH_2As-C_2H_2	Δv	−22	−26	−40
FH_2As-C_2H_4	Δv	−31	−39	−50

Conclusions

Quantum chemical calculations have been performed to study the substitution, cooperative, and solvent effects on the π pnicogen bond at the MP2/aug-cc-pVTZ level. The methyl group in the electron donor exhibits a bigger contribution to the π pnicogen bond than that in the electron acceptor. The electron-withdrawing group F in the electron acceptor leads to a larger increase in the strength of π pnicogen bond. A similar big enhancing effect is from the Li group in the electron donor. The π pnicogen bond can interplay with the hydrogen bond in the XH-FH_2Y-C_2H_4 (X=HO, NC, F; Y=P and As) trimer and both types of interactions enhanced each other. In solvent, the π pnicogen bond is also strengthened. Although it has been shown that trivalent phosphines are a common structural and enzymatic element in inorganic systems [55–57], their interaction with unsaturated hydrocarbon molecules might be important in organic systems because they are often used to synthesize some organophosphorous and organoarsenic compounds.

Acknowledgments This work was supported by the National Natural Science Foundation of China (20973149), the Outstanding Youth Natural Science Foundation of Shandong Province (JQ201006), and the Program for New Century Excellent Talents in University.

References

1. Kojić-Prodić B, Štefanić Z, Žinić M (2004) Croat Chem Acta 77:415–425
2. Knowles RR, Jacobsen EN (2010) Proc Natl Acad Sci USA 107:20678–20685
3. Desiraju GR (2010) J Chem Sci 122:667–677
4. An XL, Jing B, Li QZ (2011) Comput Theor Chem 966:278–283
5. Liao HY (2009) J Chin Chem Soc 56:532–538
6. Feng Y, Liu L, Wang JT, Li XS, Guo QX (2004) Chem Commun 40:88–89
7. Lu YX, Zou JW, Wang YH, Jiang YJ, Yu QS (2007) J Phys Chem A 111:10781–10788
8. Ammal SSC, Venuvanalingam P (1998) J Chem Phys 109:9820–9830
9. Ebrahimi A, Khorassani SMH, Delarami H, Esmaeeli H (2010) J Comput Aided Mol Des 24:409–416
10. Wheeler SE, Houk KN (2009) J Am Chem Soc 131:3126–3127
11. Bauzá A, Quiñonero D, Frontera A, Deyà PM (2011) Phys Chem Chem Phys 13:20371–20379
12. Serrano A, Castro-Vega I, Redondo M (2011) Cancers 3:1672–1690
13. Li QZ, Wu GS, Yu ZW (2006) J Am Chem Soc 128:1438–1439
14. Li QZ, Jing B, Liu ZB, Li WZ, Cheng JB, Gong BA, Sun JZ (2010) J Chem Phys 133:114303
15. Li QZ, Wang HZ, Liu ZB, Li WZ, Cheng JB, Gong BA, Sun JZ (2009) J Phys Chem A 113:1415614160
16. Faas GC, Schwaller B, Vergara JL, Mody I (2007) PloS Biol 5: e311
17. Hunter CA, Anderson HL (2009) Angew Chem Int Ed 48:7488–7499
18. Alkorta I, Blanco F, Deya PM, Elguero J, Estarellas C, Frontera A, Quinonero D (2010) Theor Chem Acc 126:1–10
19. Li QZ, Lin QQ, An XL, Gong BA, Cheng JB (2008) Chem Phys Chem 9:2265–2269
20. Li QZ, Li R, Liu ZB, Li WZ, Cheng JB (2011) J Comput Chem 32:3296–3303
21. Li R, Li QZ, Cheng JB, Liu ZB, Li WZ (2011) Chem Phys Chem 12:2289–2295
22. Jiang XN, Sun CL, Wang CS (2010) J Comput Chem 31:1410–1420
23. Escudero D, Frontera A, Quinonero D, Deya PM (2008) Chem Phys Lett 456:257–261
24. Murray JS, Riley KE, Politzer P, Clark T (2010) Aust J Chem 63:1598–1607
25. Hennemann M, Murray JS, Politzer P, Riley KE, Clark T (2012) J Mol Model. doi:101007/s00894-011-1263-5
26. Rao JS, Zipse H, Sastry GN (2009) J Phys Chem B 113:7225–7236
27. Lu YX, Li HY, Zhu X, Zhu WL, Liu HL (2011) J Phys Chem A 115:4467–4475
28. Sapse AM, Jain DC (1987) J Phys Chem 91:3923–3625
29. Li QZ, Wang NN, Yu ZW (2007) J Mol Struct (Theochem) 847:68–74
30. Murray JS, Lane P, Politer P (2007) Int J Quantum Chem 107:2286–2292
31. Politzer P, Murray JS, Clark T (2010) Phys Chem Chem Phys 12:7748–7757
32. Murray JS, Concha MC, Politzer P (2011) J Mol Model 17:2151–2157
33. Murray JS, Lane P, Politer P (2008) Int J Quantum Chem 108:2770–2781
34. Riley KE, Murray JS, Politzer P, Concha MC, Hobza P (2009) J Chem Theor Comput 5:155–163
35. Zahn S, Franck R, Hey-Hawkins E, Kirchner B (2011) Chem Eur J 17:6034–6038
36. Del Bene JE, Alkorta I, Sanchez-Sanz G, Elguero J (2011) Chem Phys Lett 512:184–187
37. Solimannejad M, Gharabaghi M, Scheiner S (2011) J Chem Phys 134:024312
38. Scheiner S (2011) J Chem Phys 134:094315
39. Scheiner S (2011) J Phys Chem A 115:11202–11209
40. Scheiner S (2011) Chem Phys 387:79–84
41. Scheiner S, Adhikari U (2011) J Phys Chem A 115:11101–11110
42. Scheiner S (2011) Phys Chem Chem Phys 13:13860–13872
43. Del Bene JE, Alkorta I, Sanchez-Sanz G, Elguero J (2011) J Phys Chem A 115:13724–13731
44. Politzer P, Murray JS, Concha MC (2008) J Mol Model 14:659–665
45. Frisch MJ, Trucks GW, Schlegel HB, Scuseria GE, Robb MA, Cheeseman JR, Montgomery JA Jr, Vreven T, Kudin KN, Burant JC, Millam JM, Iyengar SS, Tomasi J, Barone V, Mennucci B, Cossi M, Scalmani G, Rega N, Petersson GA, Nakatsuji H, Hada M, Ehara M, Toyota K, Fukuda R, Hasegawa J, Ishida M, Nakajima T, Honda Y, Kitao O, Nakai H, Klene M, Li X, Knox JE, Hratchian HP, Cross JB, Adamo C, Jaramillo J, Gomperts R, Stratmann RE, Yazyev O, Austin AJ, Cammi R, Pomelli C, Ochterski JW, Ayala PY, Morokuma K, Voth GA, Salvador P, Dannenberg JJ, Zakrzewski VG, Dapprich S, Daniels AD, Strain MC, Farkas O, Malick DK, Rabuck AD, Raghavachari K, Foresman JB, Ortiz JV, Cui Q, Baboul AG, Clifford S, Cioslowski J, Stefanov BB, Liu G, Liashenko A, Piskorz P, Komaromi I, Martin RL, Fox DJ, Keith T, Al-Laham MA, Peng CY, Nanayakkara A, Challacombe M, Gill PMW, Johnson B, Chen W, Wong MW, Gonzalez C, Pittsburgh PA, Pople JA (2009) Gaussian 09, Revision A02. Gaussian Inc, Wallingford, CT
46. Boys SF, Bernardi F (1970) Mol Phys 19:553–566
47. Tomasi J, Persico M (1994) Chem Rev 94:2027–2094
48. Glendening ED, Reed AE, Carpenter JE, Weinhold F (2011) NBO Version 31
49. Bukowski R, Cencek W, Jankowski P, Jeziorski B, Jeziorska M, Kucharski SA, Misquitta AJ, Moszynski R, Patkowski K, Rybak S, Szalewicz K, Williams HL, Wormer PES (2003) SAPT2002: An Ab initio program for many-body symmetry-adapted perturbation theory calculations of intermolecular interaction energies sequential and parallel versions
50. Bulat FA, Toro-Labbé A, Brinck T, Murray JS, Politzer P (2010) J Mol Model 16:1679–1691
51. Li QZ, Wang NN, Yu ZW (2008) J Mol Struct (Theochem) 862:74–79
52. Cheng JB, Li R, Li QZ, Jing B, Liu ZB, Li WZ, Gong BA, Sun JZ (2010) J Phys Chem A 114:10320–10325
53. Scheiner S (2011) J Chem Phys 134:164313
54. Wang ZX, Duan YJ (2005) Theor Comput Chem 4:SI 689–705
55. Crestani MG, Manbeck GF, Brennessel WW, McCormick TM, Eisenberg R (2011) Inorg Chem 50:7172–7188
56. Hu J, Nguyen MH, Yip JHK (2011) Inorg Chem 50:7429–7439
57. Platel RH, White AJP, Williams CK (2011) Inorg Chem 50:7718–7728